SUPPORTING INFORMATION

Mechanical Counterbalance of Kinesin and Dynein Motors in Microtubular Network Regulates Cell Mechanics, 3D Architecture, and Mechanosensing

Alexander S. Zhovmer [1,*], Alexis Manning [1,#], Chynna Smith [2,#], James. B. Hayes [3,#], Dylan T. Burnette [3], Jian Wang [4], Alexander X. Cartagena-Rivera [2,*], Nikolay V. Dokholyan [4,5,*], Rakesh K. Singh [6,*], and Erdem D. Tabdanov [4,*]

Affiliations:

1 - Center for Biologics Evaluation and Research, U.S. Food and Drug Administration, Silver Spring, MD, 20903, USA
2 - Section on Mechanobiology, National Institute of Biomedical Imaging and Bioengineering, National Institutes of Health, Bethesda, MD, 20892, USA
3 - Department of Cell and Developmental Biology, Vanderbilt Medical Center, University of Vanderbilt, Nashville, TN, 37232, USA
4 - Department of Pharmacology, Penn State College of Medicine, Pennsylvania State University, Hummelstown, PA, 17036, USA
5 - Department of Biochemistry & Molecular Biology, Penn State College of Medicine, Pennsylvania State University, Hershey, PA, 17033, USA
6 - Department of Obstetrics and Gynecology, University of Rochester Medical Center, Rochester, NY, 14620, USA

# - These authors contributed equally

* - **Correspondence authors:**

Alexander S. Zhovmer, Tel: 1-301-402-1606; alexander.zhovmer@fda.hhs.gov
Alexander X. Cartagena-Rivera: Tel: 1-301-503-4033; alexander.cartagena-rivera@nih.gov
Nikolay V. Dokholyan: dokh@psu.edu
Rakesh K. Singh, Tel: 1-585-276-6281; rakesh_singh@urmc.rochester.edu
(Lead contact): Erdem D. Tabdanov, Tel: 1-717-531-0003 Ext: 4430; ekt5171@psu.edu

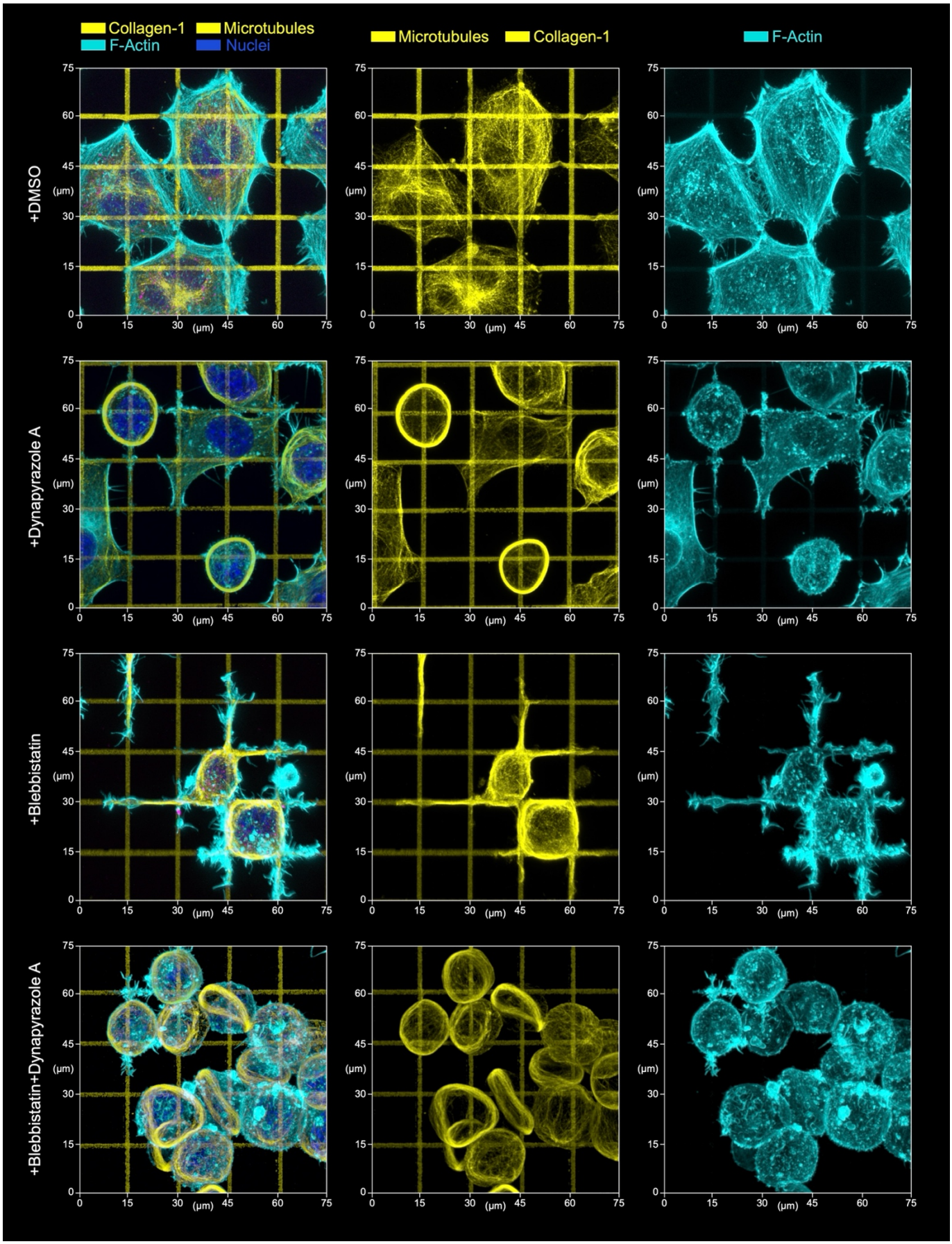
Collagen-1
Microtubules
F-Actin
Nuclei
Microtubules
Collagen-1
F-Actin
+DMSO
+Dynapyrazole A
+Blebbistatin
+Blebbistatin+Dynapyrazole A
(μm)
0
15
30
45
60
75

SI1. Top 3D overview of MDA-MB-231 cells during their adhesion and spreading along the artificial extracellular matrix (orthogonal collagen grid, G'=50 kPa). Corresponds to Figure 1a. Micrographs present cell configurations in the control condition **(+DMSO)**, during dynein inhibition **(+Dynapyrazole A)**, in the presence of actomyosin contractility inhibitor **(+Blebbistatin)**, and under combined dynein and actomyosin contractility suppression **(+Blebbistatin+Dynapyrazole A)**. Upon biaxial spreading along the orthogonal collagen lanes in the control conditions **(+DMSO)** cells develop a polygonal architecture with stress-fibers predominantly developing at the mechanically tensed cell periphery - *i.e.*, concave free cell edges. Suppression of the dynein motor protein activity **(+Dynapyrazole A)** results in cell spreading architecture disarray, reduced polygonal cell architectures and partially 'dendritic'-like cell morphologies (see also **Figure 3c, +Dynapyrazole A**). Actomyosin contractility inhibition **(+Blebbistatin)** shifts cell cytoskeletal organization towards the spreading network of dendritic protrusions that compliantly extend along the collagen grid with high cell dendrites-to-grid structural fidelity. These dendritic protrusions have the microtubule scaffold as their core. Notably, combined dynein and myosin II inhibition **(+Blebbistatin+Dynapyrazole A)** results in the suppressed cell spreading (but not adhesion), and formation of MT rings that deform non-spread spheroid cells into the lenticular discoids.
F-actin is labelled with Phalloidin-ATTO 647N. Chromatin is labelled with Hoechst.

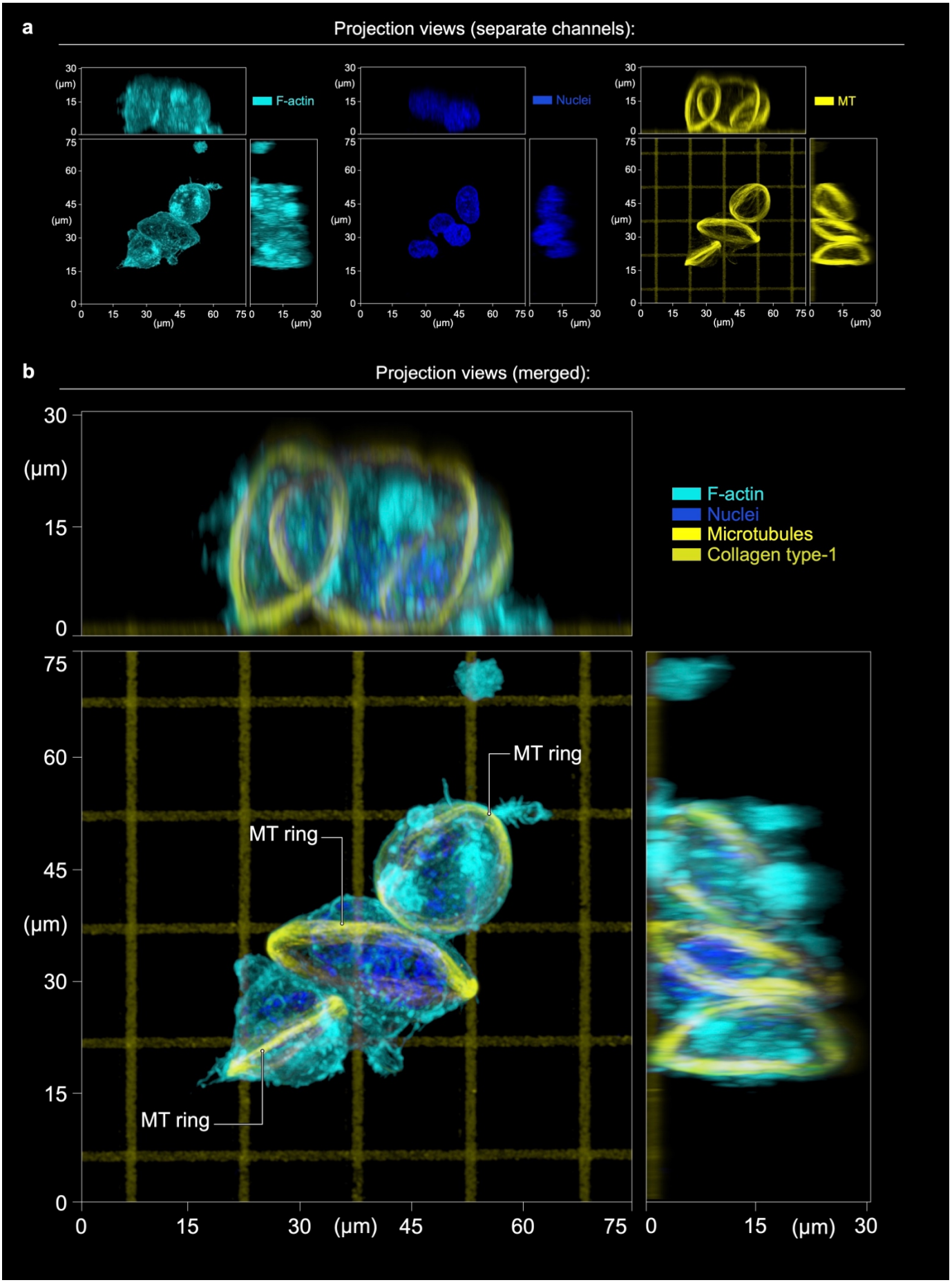
a
Projection views (separate channels):
F-actin
Nuclei
MT
(μm)
b
Projection views (merged):
F-actin
Nuclei
Microtubules
Collagen type-1
MT ring
MT ring
MT ring

SI2. Detailed projection views of discoid MDA-MB-231 cells that were formed during +Dynapyrazole A+Blebbistatin treatment (corresponds to Figure 1b and 1c).

(a) - Separate channel 3D projection views: F-actin (phalloidin), nuclei (Hoechst), microtubules (tubulin immunofluorescence imaging), collagen type-1 micropatterned grids (prelabeled).

(b) - Enlarged and detailed 2D projection views of the merged channels.

F-actin is labelled with Phalloidin-ATTO 647N. Chromatin is labelled with Hoechst.

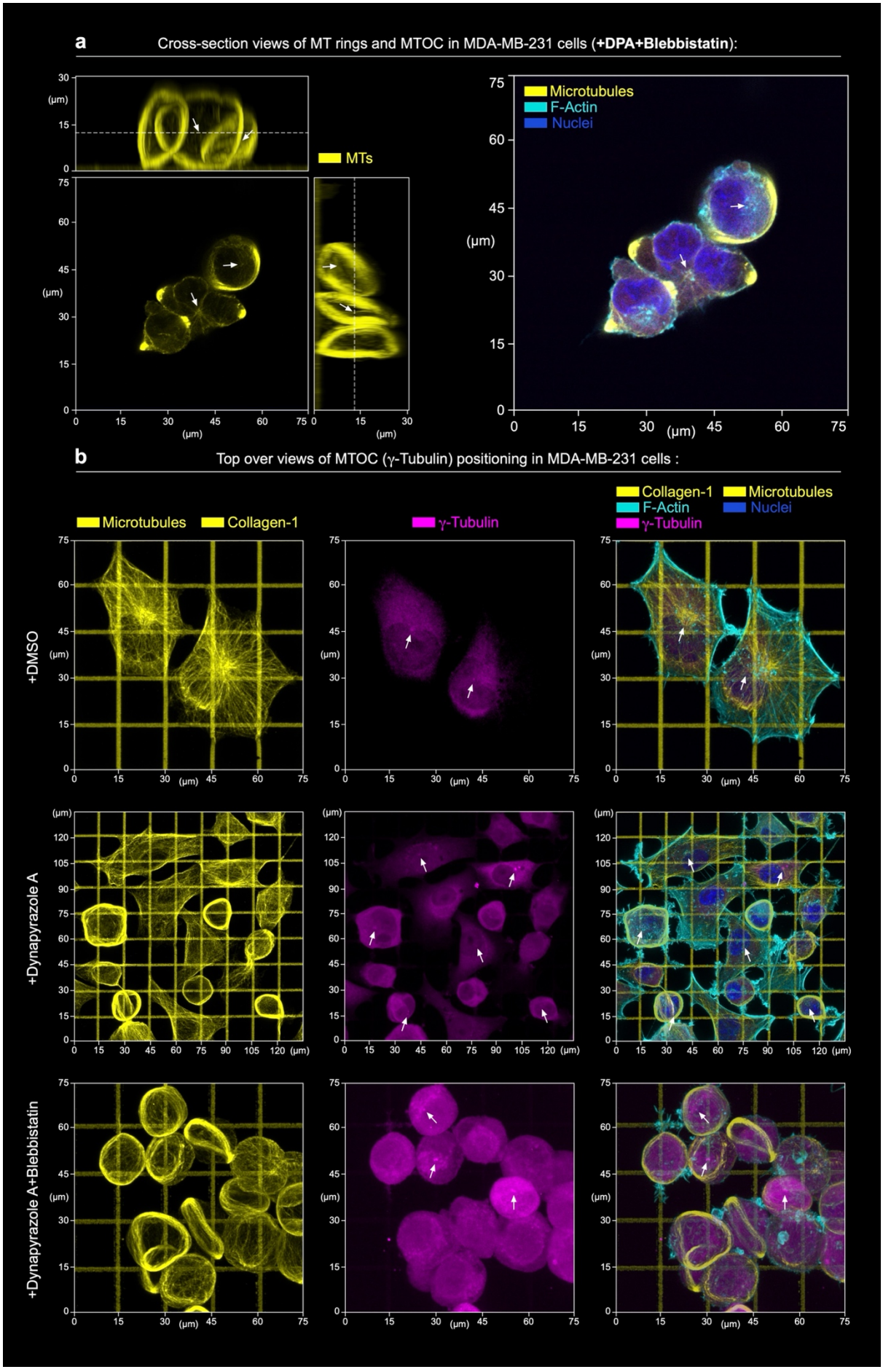
a
Cross-section views of MT rings and MTOC in MDA-MB-231 cells (+DPA+Blebbistatin):
MTs
Microtubules
F-Actin
Nuclei
(µm)
b
Top over views of MTOC (γ-Tubulin) positioning in MDA-MB-231 cells :
Microtubules
Collagen-1
γ-Tubulin
Collagen-1
Microtubules
F-Actin
Nuclei
γ-Tubulin
+DMSO
+Dynapyrazole A
+Dynapyrazole A+Blebbistatin

SI3. MTOC positioning perturbation by Dynapyrazole A±Blebbistatin treatments in MDA-MB-231 cells.
(a) - MTOCs (*arrows*) do not display spatial association with the mature MT rings in the discoid cells in **+Dynapyrazole A+Blebbistatin**, as shown by the cell's structure medial cross-sections (*shown with dashed lines*) of the MDA-MB-231 cells.
(b) - γ-Tubulin-positive foci (MTOC, *arrows*), shown *via* fluorescent immunocytochemical microscopy analysis in control cells (+DMSO), during dynein inhibitor (**+Dynapyrazole A**), and during combined dynein and myosin II suppression (**+Dynapyrazole A+Blebbistatin**).
*Note that MTOCs canonically localize predominantly with the MT radial array's convergence foci in control cells (**+DMSO**).* Upon dynein inhibition the MT networks lose their pronounced radial array architecture in favor of the ring-like bands formation at the cell cortex, while MTOCs translocate to the random locations within cytosol (**+Dynapyrazole A**). In **+Dynapyrazole A+Blebbistatin**-treated cells, and after the complete MT network reorganization, the γ-Tubulin foci (MTOCs, *arrows*) do not spatially associate with the MT rings.

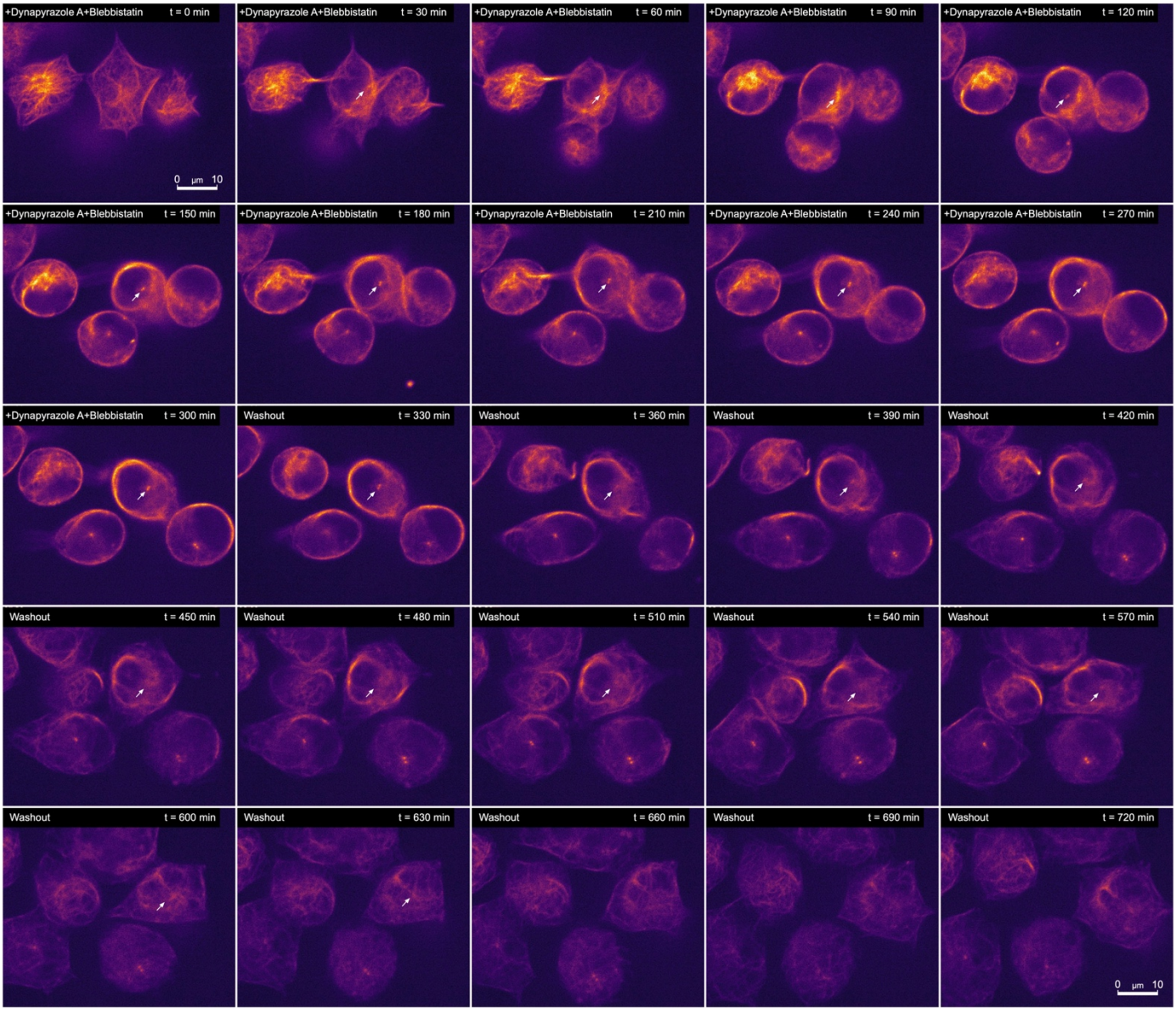

SI4. Dynapyrazole A+Blebbistatin-dependent MT ring formation and inhibition of cell spreading is reversible upon washout of Dynapyrazole A+Blebbistatin-containing media. Time-course images (30 min-long steps) of MDA-MB-231 cells de-adhesion and MTs redistribution (*live SiR tubulin staining, cells equatorial cross-section views*), accompanied with the MT ring formation (*i.e.,* circumferential MT redistribution) upon addition of the **+Dynapyrazole A+Blebbistatin** mixture to the spread polygonal cells (collagen type-1 grid is not shown), at the time t=0 min. Washout of the **+Dynapyrazole A+Blebbistatin** mixture (t=330 min) with the fresh preheated (37ºC) and CO_2-preincubated cell culture medium reverses MT ring formation resulting in redistribution of MTs into a radial architecture, accompanied by the cell re-spreading back into the polygonal architectures. *Note the MTOC segregation from the MT rings (arrows).*

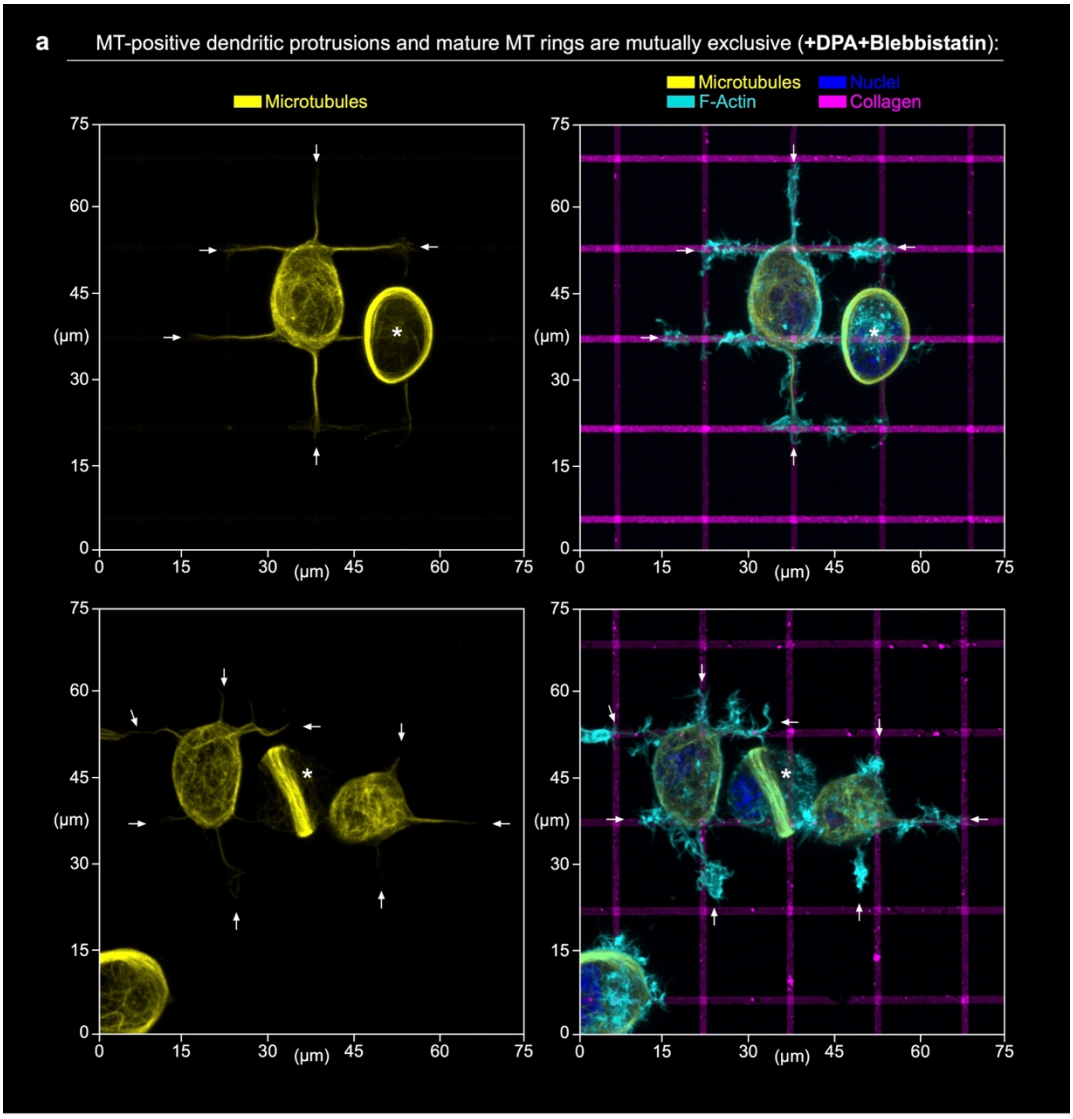
a
MT-positive dendritic protrusions and mature MT rings are mutually exclusive (+DPA+Blebbistatin):
Microtubules
Microtubules
Nuclei
F-Actin
Collagen
(μm)
0
15
30
45
60
75

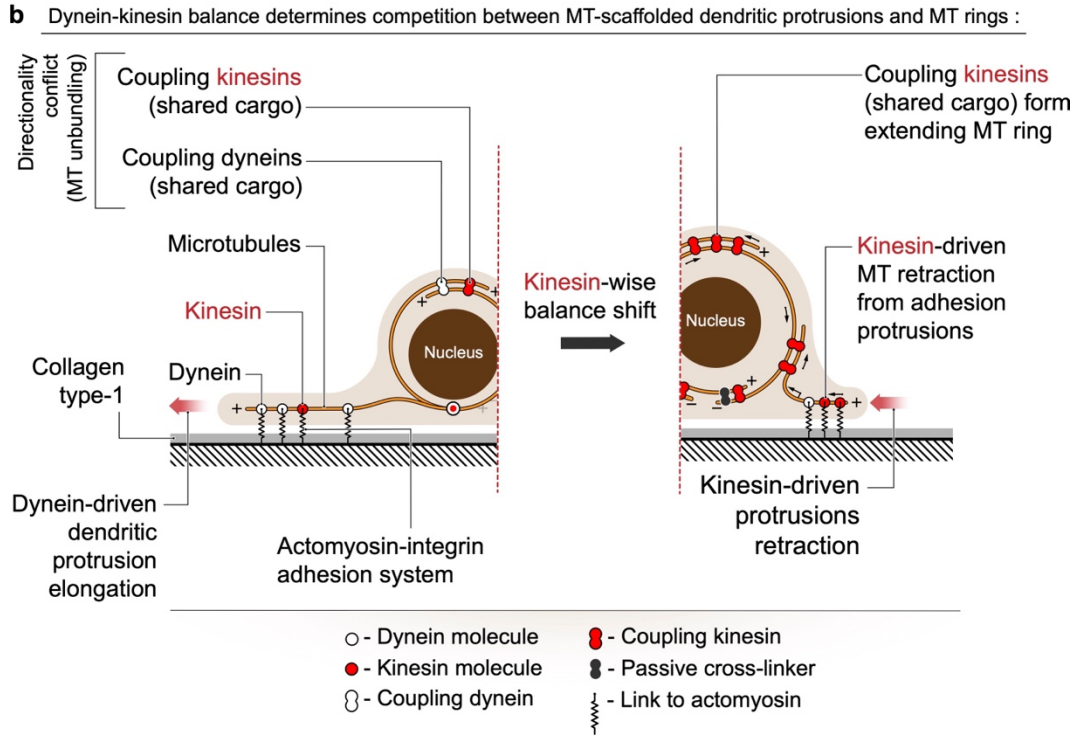
b
Dynein-kinesin balance determines competition between MT-scaffolded dendritic protrusions and MT rings :
Directionality conflict (MT unbundling)
Coupling kinesins (shared cargo)
Coupling dyneins (shared cargo)
Microtubules
Kinesin
Dynein
Collagen type-1
Nucleus
Dynein-driven dendritic protrusion elongation
Actomyosin-integrin adhesion system
Kinesin-wise balance shift
Coupling kinesins (shared cargo) form extending MT ring
Kinesin-driven MT retraction from adhesion protrusions
Kinesin-driven protrusions retraction
- Dynein molecule
- Kinesin molecule
- Coupling dynein
- Coupling kinesin
- Passive cross-linker
- Link to actomyosin

SI5. MT-containing dendritic protrusions and MT rings are mutually exclusive in MDA-MB-231 cells.
(a) - During the 1 hour-long course of **+Dynapyrazole A+Blebbistatin** treatment cells display a transitioning from the collagen grid-guided MT-positive dendritic protrusions (*arrows*) towards the mature 3D MT rings (*asterisks*).
(b) - Suggested mechanism for the mutual exclusivity between the MT-scaffolded dendritic protrusions and the mature MT rings includes dyneins as the motors that drive the microtubules along the collagen adhesion lanes into the growing protrusions, promoting the cell spreading and dendritic protrusions elongation. Kinesin-wise dynein-kinesin balance shift leads to the kinesin-driven (kinesin-1) microtubule retraction from the cell protrusions, and MTs redistribution into the MT rings. *Note that after 1 hour-long **+Dynapyrazole A+Blebbistatin**-treatment each cell either demonstrates the mature MT rings (~65% of the cell population, n=100) or the dendritic protrusions (~35%, n=100), but not both.*

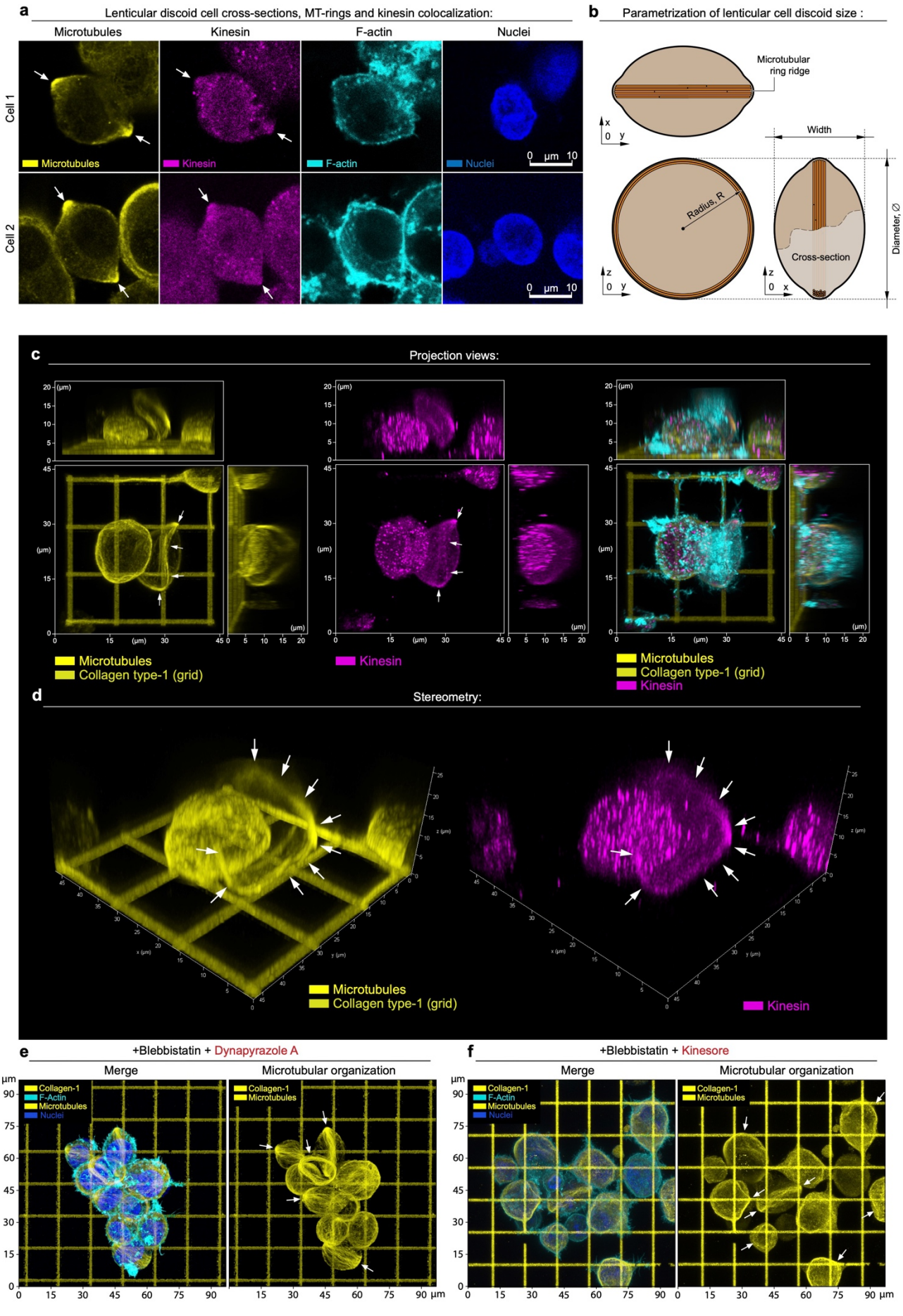
a
Lenticular discoid cell cross-sections, MT-rings and kinesin colocalization:
Microtubules
Kinesin
F-actin
Nuclei
Cell 1
Cell 2
0 µm 10
b
Parametrization of lenticular cell discoid size :
Microtubular ring ridge
Width
Radius, R
Cross-section
Diameter, ∅
c
Projection views:
Microtubules
Collagen type-1 (grid)
Kinesin
d
Stereometry:
e
+Blebbistatin + Dynapyrazole A
Merge
Microtubular organization
Collagen-1
F-Actin
f
+Blebbistatin + Kinesore

SI6. Details of structural dissection of the MT ring composition.
(a) - Detailed channel-separated views of discoid cell median cross-sections (*cell 1 and cell 2*). Corresponds to **Figure 3a**.
(b) - Detailed schematic of the discoid cell structural parameters measurement (width *vs.* diameter). Corresponds to **Figure 3b**.
(c, d) - Standard 2D projection views **(c)**, and stereometric views of the MT ring and the kinesin immunofluorescent spatial distribution **(d)**, showing kinesin colocalization with the **+Dynapyrazole A+Blebbistatin**-induced MT rings (*arrows*). Corresponds to **Figure 3a**.
(e, f) - Detailed, channel-separated view of the MT rings (*arrows*) in **+Dynapyrazole A+Blebbistatin (e)**, as compared to the alternative kinesin outbalance induction *via* **+Kinesore+Blebbistatin** treatment **(f).** MT rings are outlined by arrows. Corresponds to **Figure 3e**. F-actin is labelled with Phalloidin-ATTO 647N. Chromatin is labelled with Hoechst.

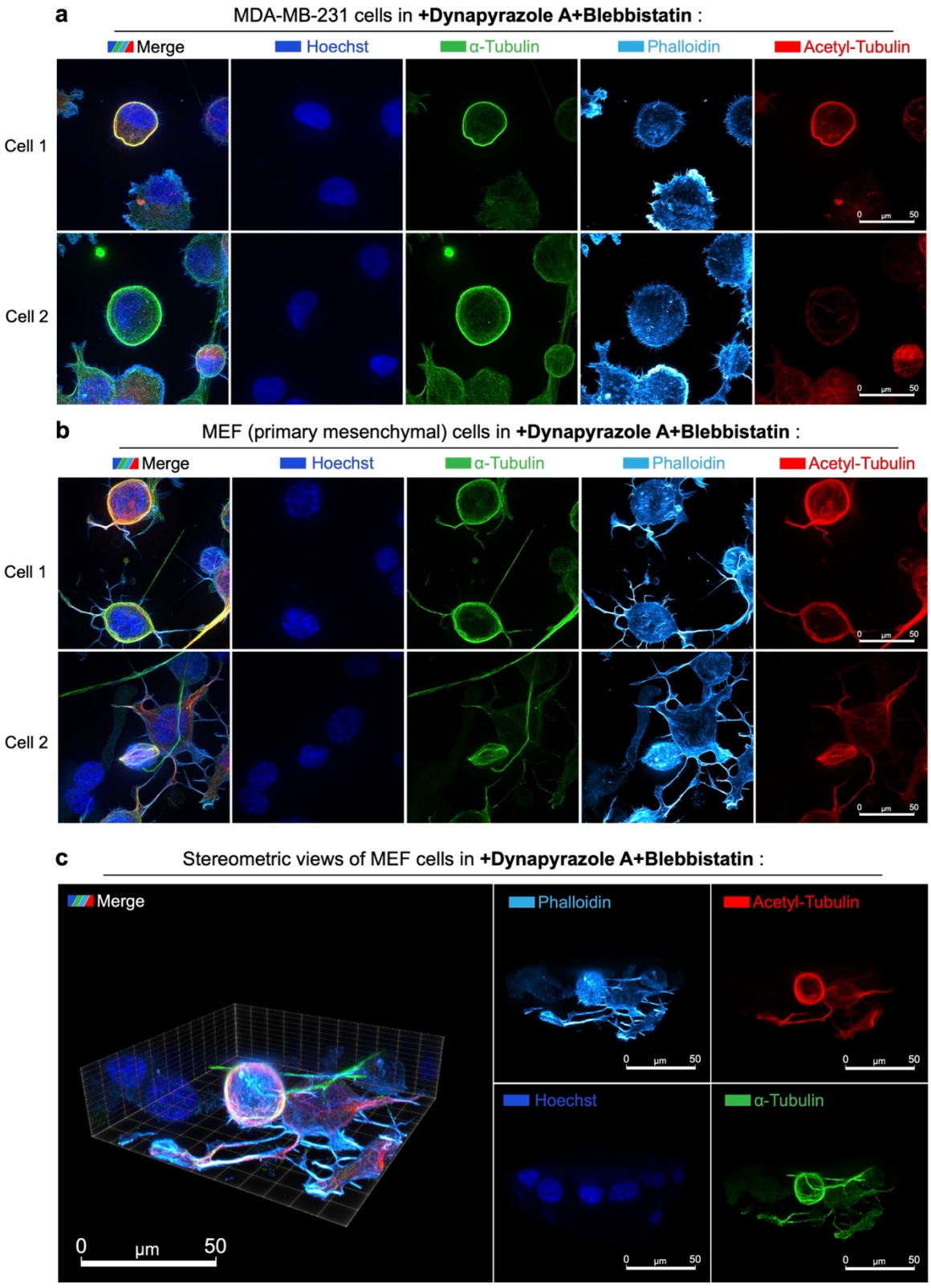

SI7. Acetylated microtubules are incorporated into the MT rings along with the non-modified MTs in both MDA-MB-231 and in the primary mesenchymal MEF cells in response to +Dynapyrazole A+Blebbistatin treatment. **(a)** - MDA-MB-231 cells, and **(b)** MEF cells both display MT circumferential band (ring) formation that feature both non-modified and acetylated α-Tubulin. *Note that if cells do not feature strong MT acetylation, cells still form the MT rings.* **(c)** - Stereometric views of the cell 2 (MEF), shown on (b).

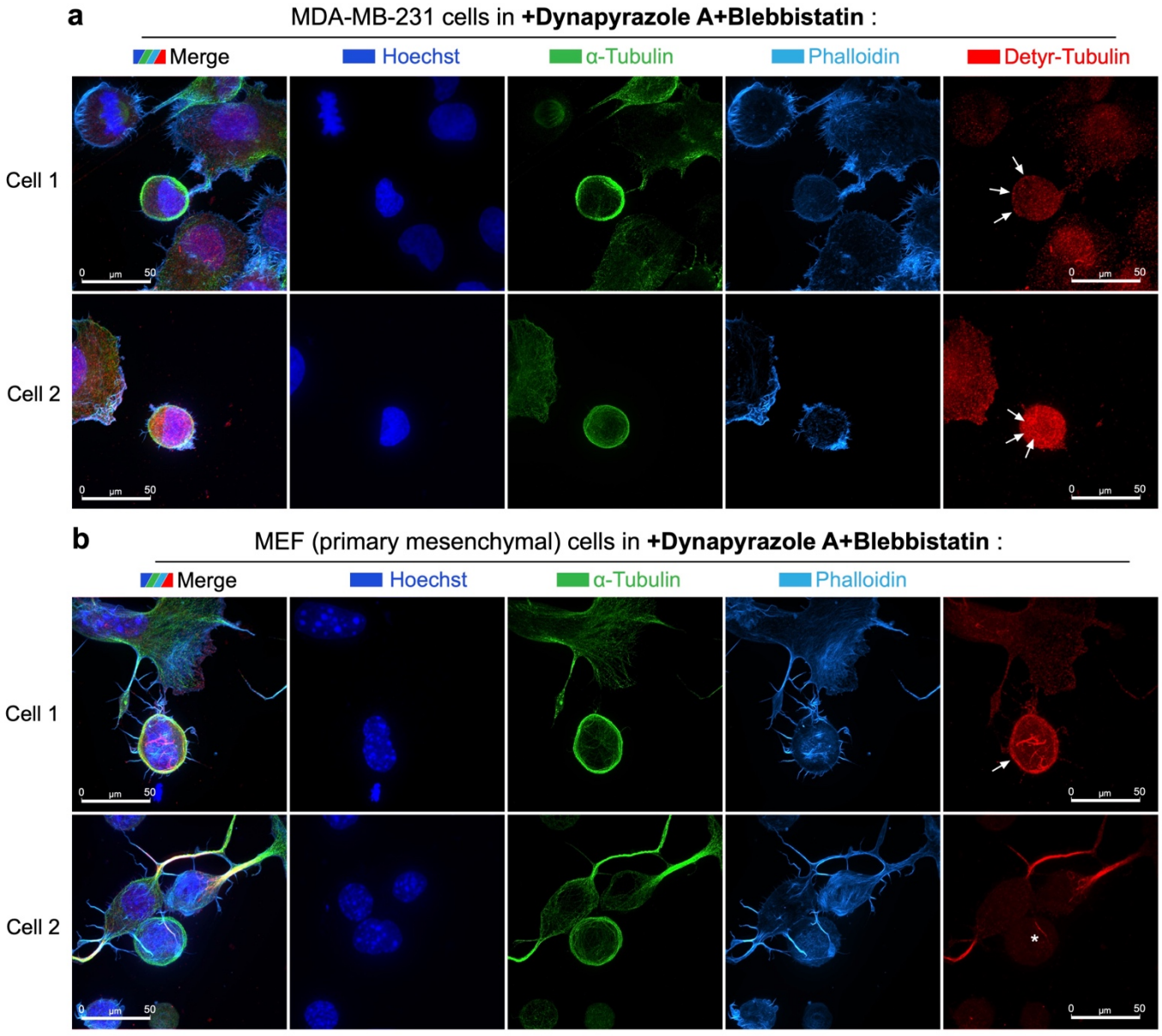

SI8. Detyrosinated microtubules are incorporated into the MT rings along with the non-modified MTs in both MDA-MB-231 and in the primary mesenchymal MEF cells in response to +Dynapyrazole A+Blebbistatin treatment.

(a) - MDA-MB-231 cells, and **(b)** MEF cells both display MT circumferential band (ring) formation that feature both non-modified and detyrosinated (*arrows*) α-Tubulin. *Note that if cells do not feature strong MT detyrosination (asterisk), cells still form the MT rings.*

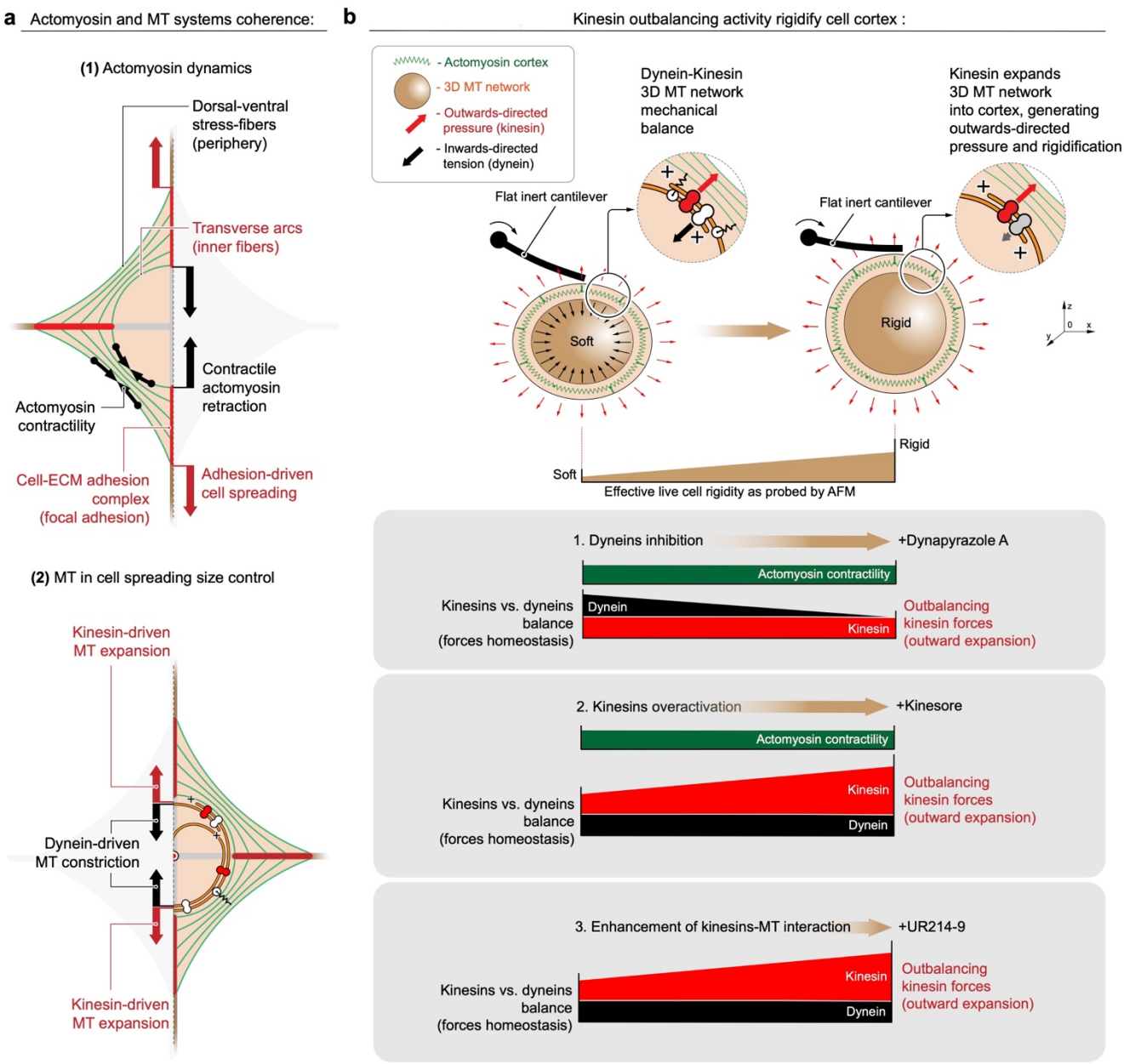

SI9. Dynein-kinesin balance controls cell size during spreading, as well as cell rigidity.
(a) - MDA-MB-231 cell spreading on collagen-1 orthogonal grid (biomimetic ECM) is a result of mechanical superposition of **(1)** contractile actomyosin cytoskeleton adhesion system (stress-fibers+focal adhesions), and **(2)** collagen "fibers" organize the cell mechanical dynamics into a balanced cell spreading process and cell contractile MT network expansion-contraction, driven by kinesin-dynein counterbalancing activity. Corresponds to **Figure 3d**.
(b) - Alternative cell rigidification mechanisms: (*Top*) - Schematics of the cell rigidification, driven by kinesin-wise activity outbalance over dyneins that leads to the kinesin-driven mechanical expansion of the MT network into the cell cortex. (*Bottom*) - **(1)** Dynein inhibition with Dynapyrazole A, Kinesin overactivation with Kinesore **(2)**, as well as with septin-9-MT complex, induced by UR214-9 septin filaments disassembly **(3)** all lead to the dynein-kinesin activity balance shift towards kinesins, leading to the similar final effects of the cell cortex rigidification, detected by AFM. Corresponds to **Figure 4c**.

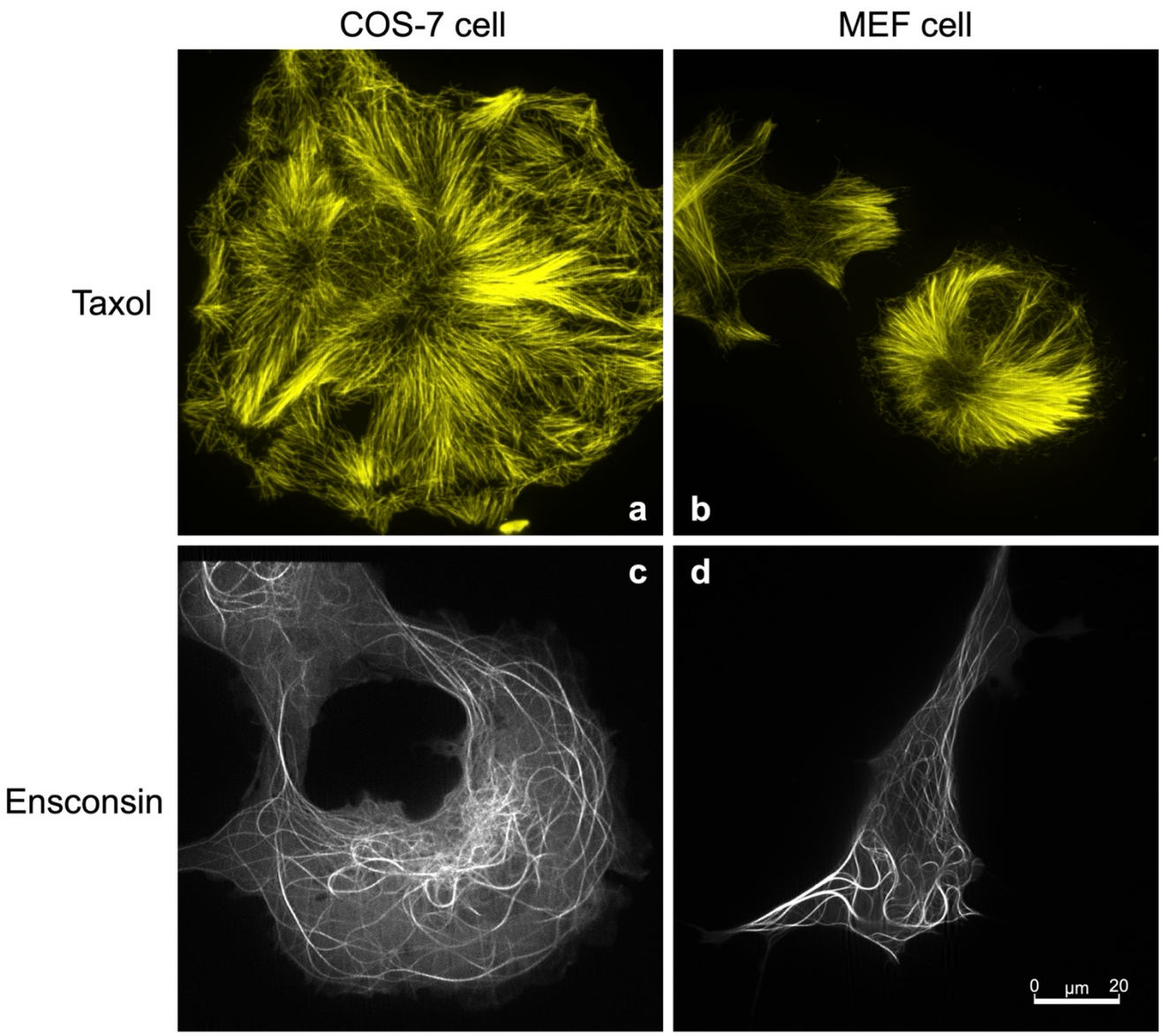

SI10. Microtubules stabilization alone does not induce MT rings formation.
Taxol-stabilized microtubules are incorporated into the MT bundles in both MDA-MB-231 **(a)** and in the primary mesenchymal MEF cells **(b)**. However, neither (a) - MDA-MB-231 cells, nor (b) MEF cells form MT rings within an acute experiment. MDA-MB-231 and MEF cells transfected with microtubule binding domain of ensconsin (EMTB-3×GFP) display formation of prominent MT bundles, however these MT bundles neither coalesce into MT ring nor induce discoid cell deformation. β-tubulin staining in panels (a) and (b), live GFP imaging in panels (c) and (d). All imaging is performed with iSIM microscopy.

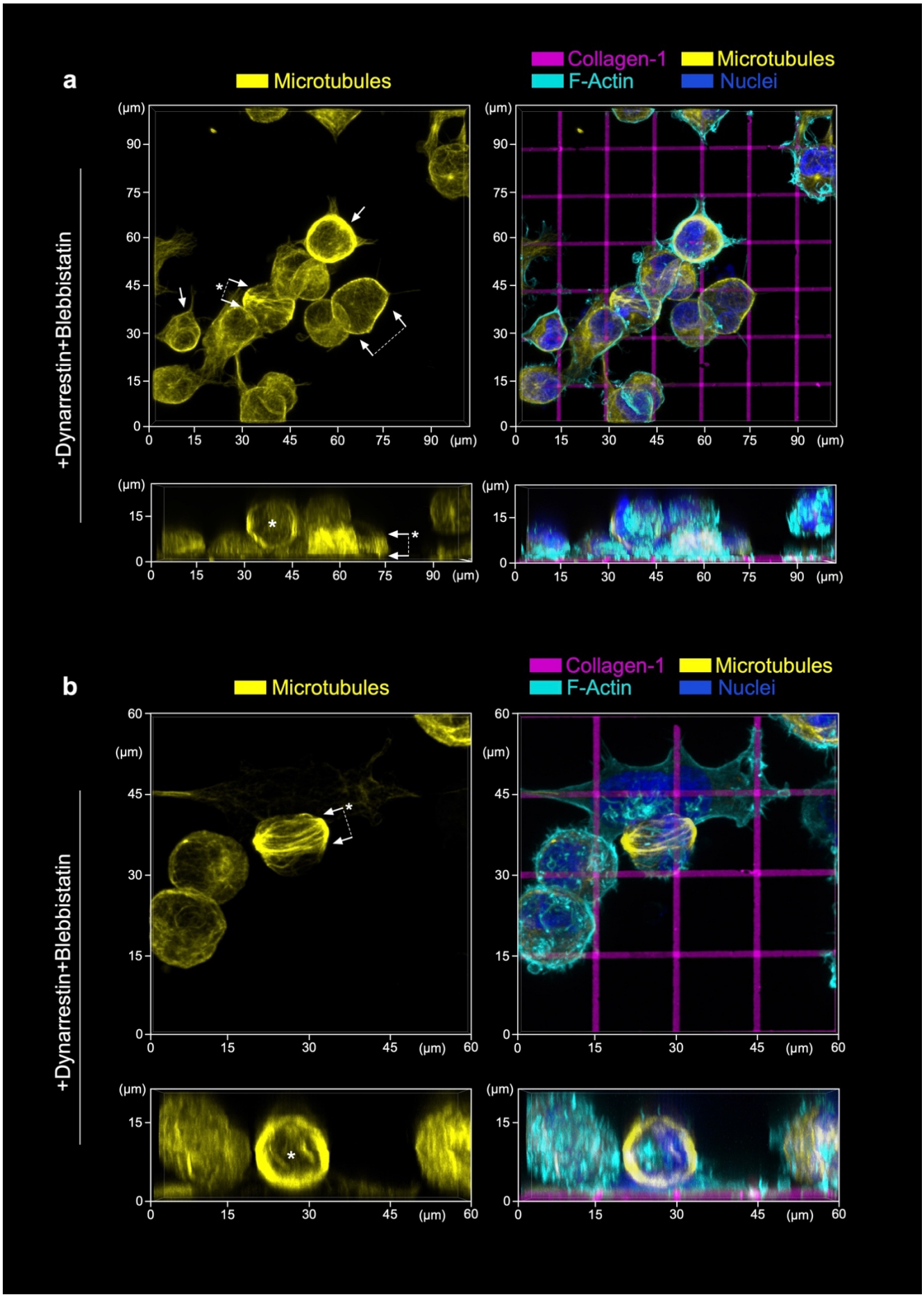
a
Microtubules
Collagen-1
Microtubules
F-Actin
Nuclei
+Dynarrestin+Blebbistatin
(µm)
0
15
30
45
60
75
90
b
Microtubules
Collagen-1
Microtubules
F-Actin
Nuclei
+Dynarrestin+Blebbistatin
(µm)
0
15
30
45
60

SI11. Dynein inhibition with 50 μM Dynarrestin (+Dynarrestin+Blebbistatin) is less effective at MT network reorganization into the MT rings and cell discoid deformation.

(a) - MDA-MB-231 cell spreading on collagen-1 orthogonal grid after 1 hour of incubation in **+Dynarrestin+Blebbistatin** display MT rings at the various stages of structural maturity (*arrows*). A mature MT ring (*asterisk*) displays a poor lateral condensation.

(b) - A detailed capture of the MDA-MB-231 cell with a mature MT ring (*asterisk*).

F-actin is labelled with Phalloidin-ATTO 647N. Chromatin is labelled with Hoechst.

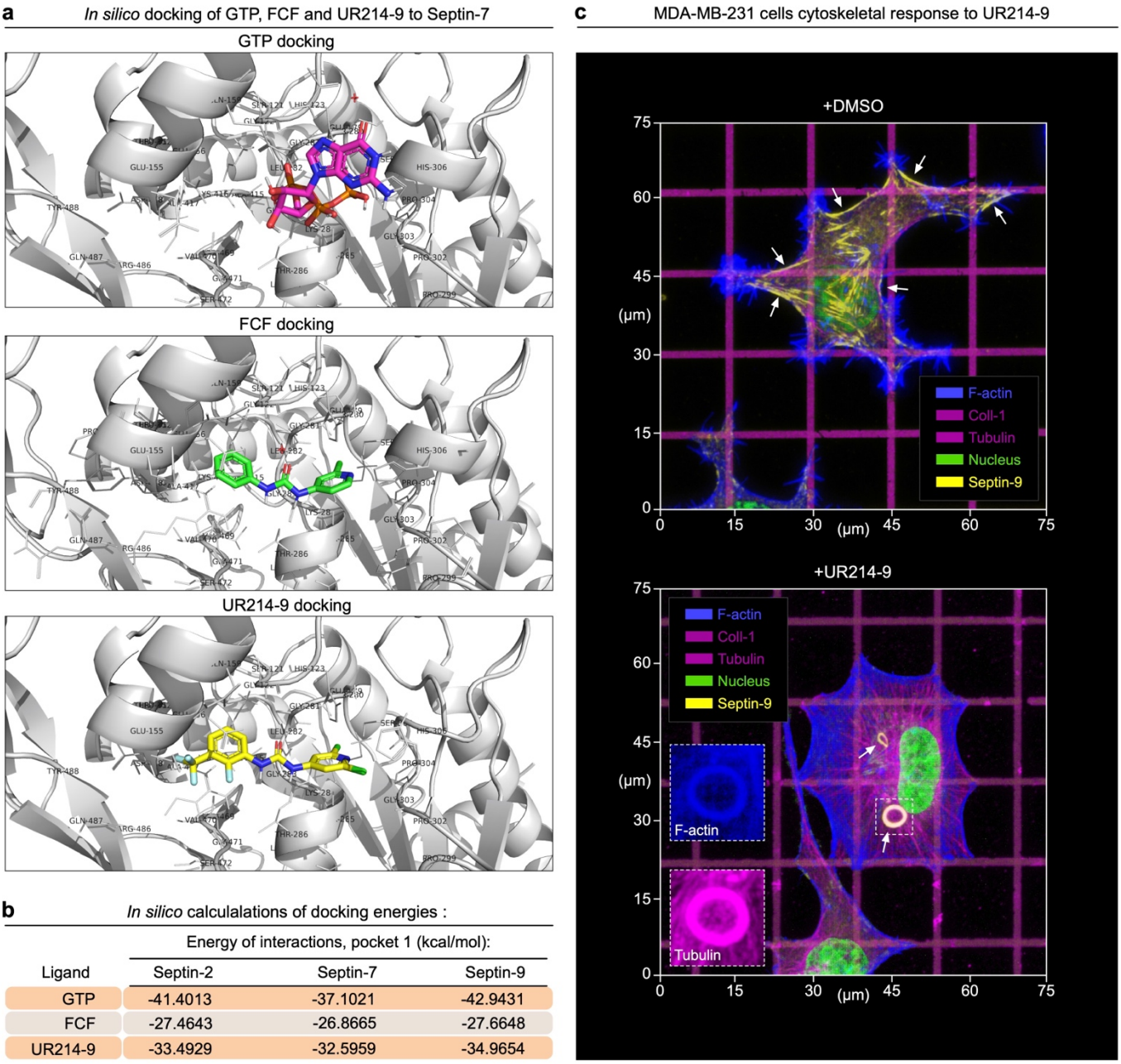

b *In silico* calculalations of docking energies :

Ligand	Energy of interactions, pocket 1 (kcal/mol): Septin-2	Septin-7	Septin-9
GTP	-41.4013	-37.1021	-42.9431
FCF	-27.4643	-26.8665	-27.6648
UR214-9	-33.4929	-32.5959	-34.9654

SI12. UR214-9-septin *in silico* docking simulations display competitive energies of interactions as compared to FCF, GTP and GDP, and feature a strong septin filaments disassembly effects in adhesive contractile cells.

(a) - *In silico* computational model for UR214-9 docking to septin-7's GTPase site, as compared to FCF inhibitor and GTP.

(b) - *In silico*-calculated energies of interactions between septin-2, septin-7 or septin-9 and GTP, FCF or UR214-9. *Note the UR214-9 docking energy is more optimized and closer mimics GTP, than FCF septin inhibitor.*

(c) - Septin (septin-9) cytoskeleton reorganization in well-spread MDA-MB-231 cells in response to UR214-9 treatment, 1 hour treatment.

*Note septin-9 translocation from the peripheral stress-fibers at the free cell edges (**+DMSO**, arrows) that accumulate most of the tensile energy in control contractile cells, towards microtubules (**+UR214-9**, arrows). UR214-9-induced septins blockade leads to the MT network density buildup **(+UR214-9)** in comparison to the control cells **(+DMSO)**,*

microtubular filament enrichment with F-actin (boxed inserts), and MT coiling into the subcellular size 2-5 μm rings, indicating the active motor participation in the rings formation, as opposed to the passive MT bundling at the spatially constraining boundaries of the cell, such as cell cortex during MT overstabilization and excessive passive cross-linking. Note that septin-7 and other isoforms also translocate from F-actin to cytosol upon UR214-9 treatment (not shown).

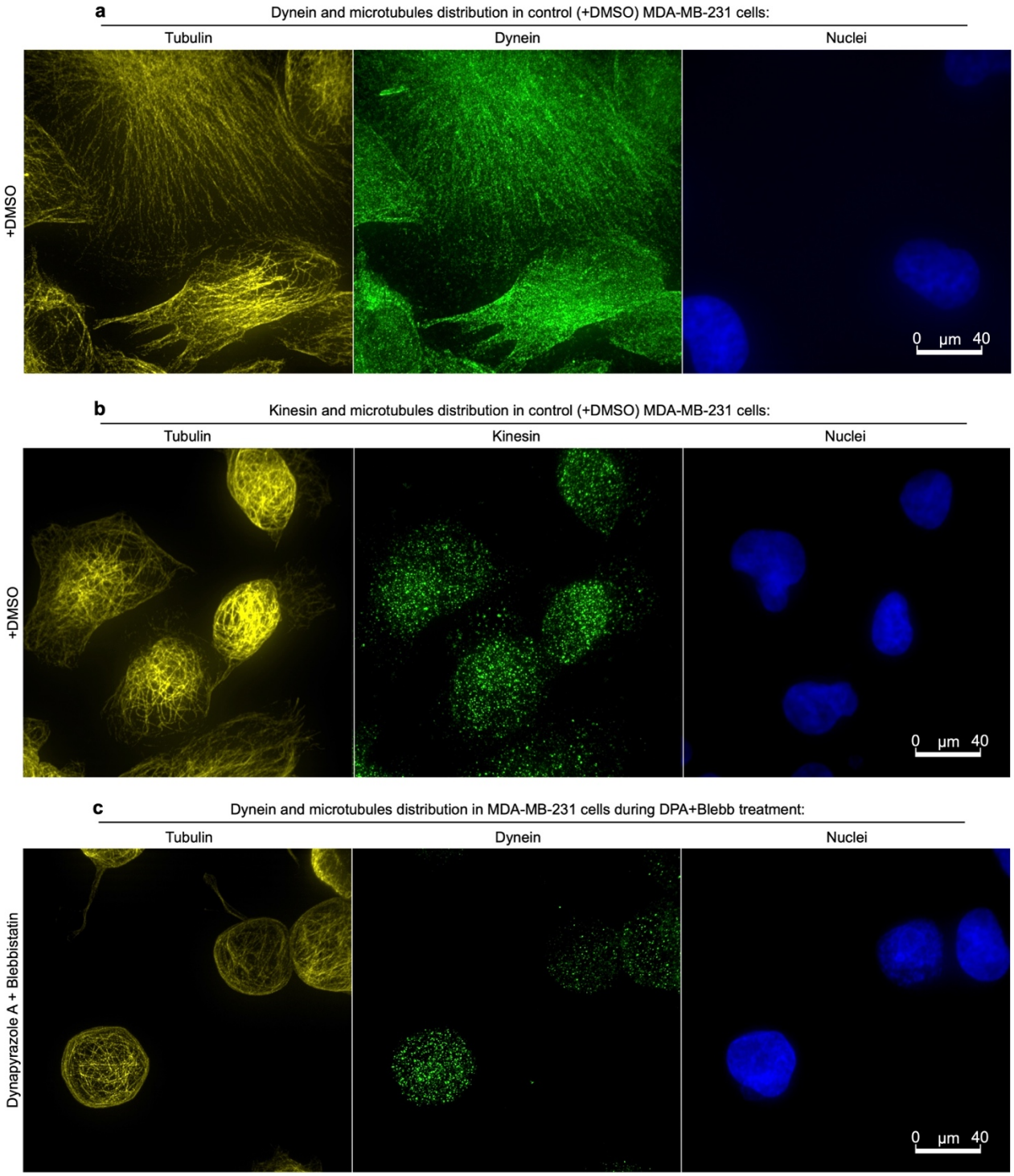

SI13. Localization of dyneins and kinesins in control conditions (+DMSO), and during +Dynapyrazole A+Blebbistatin treatments.

(a) - Dyneins colocalize with the MT network in **+DMSO**. Corresponds to **Figures 3a, 4b**.

(b) - Kinesins show diffuse distribution throughout cell volume in DMSO, but shows strong MT ring colocalization in **+Dynapyrazole A+Blebbistatin**, see **Figure 3a** and **SI3a, SI3c, and SI3d**. Corresponds to **Figure 3a, 4b**.

(c) - **Dynapyrazole A+Blebbistatin** treatment induces dynein-MT dissociation, dynein translocation from MT network into cytoplasm. Chromatin is labelled with Hoechst.

Corresponds to **Figure 3a.**

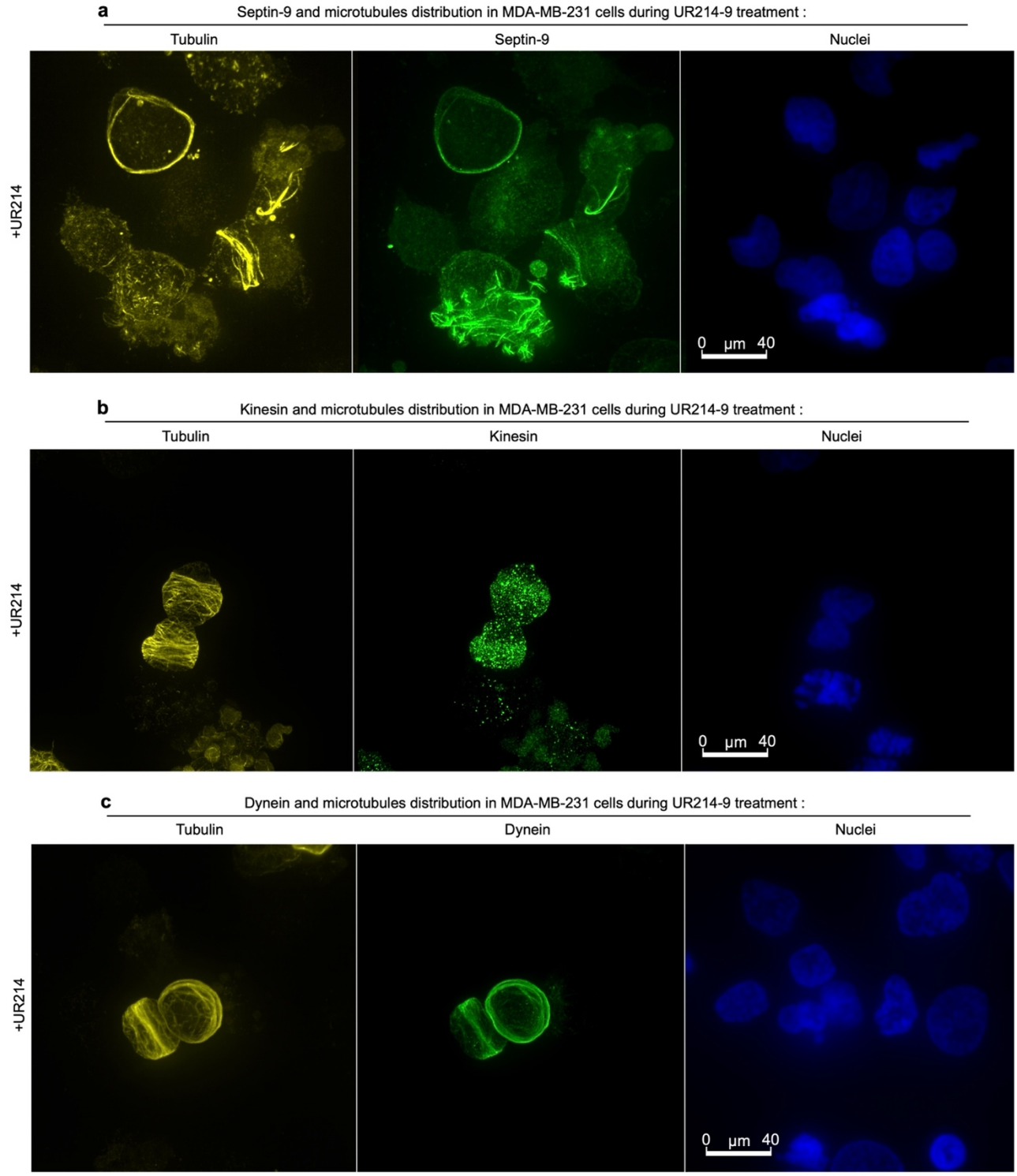

SI14. Dyneins, kinesins and septin-9 localization in MDA-MB-231 cells during UR214-9 treatment.
(a) - Septin-9 localizes at MT network in **+UR214-9** conditions.
(b) - Kinesins colocalize with forming MT rings during microtubule translocation of septin-9 in UR214-9 treatment.
(c) - Dyneins colocalize with MT network during UR214-9 treatment, since UR214-9 overactivates kinesins, but does not suppress dyneins.
Corresponds to **Figures 4b**, **4d**, and **4e**.
Chromatin is labelled with Hoechst.